Enlai Gao[1]
Department of Engineering Mechanics,
School of Civil Engineering,
Wuhan University,
Wuhan, Hubei 430072, China
e-mail: enlaigao@whu.edu.cn

Xiangzheng Jia
Department of Engineering Mechanics,
School of Civil Engineering,
Wuhan University,
Wuhan, Hubei 430072, China
e-mail: 2016301890019@whu.edu.cn

Langquan Shui[1]
Department of Engineering Mechanics,
School of Civil Engineering,
Wuhan University,
Wuhan, Hubei 430072, China
e-mail: l.q.shui@whu.edu.cn

Ze Liu
Department of Engineering Mechanics,
School of Civil Engineering,
Wuhan University,
Wuhan, Hubei 430072, China
e-mail: ze.liu@whu.edu.cn

Tuning the Nonlinear Mechanical Anisotropy of Layered Crystals via Interlayer Twist

Multilayer graphene exhibits strong mechanical anisotropy in the nonlinear elastic regime, and tuning this mechanical anisotropy without damaging the graphene is a tough challenge. In this work, we propose an efficient strategy to tune the mechanical anisotropy of multilayer graphene via interlayer twist. The orientation-dependent strain–stress curve of monolayer graphene is described in analytical form, which is further generalized for predicting the mechanical anisotropy of twisted multilayer graphene by introducing a twist-induced "phase shift." These predictions are supported by atomistic simulations. It is found that the strong nonlinear mechanical anisotropy of multilayer graphene can be effectively tuned and even eliminated via the twist-induced phase shift. These findings are finally generalized for other layered crystals. [DOI: 10.1115/1.4048647]

Keywords: mechanical anisotropy, twisted graphene, twisted bilayer, mechanical properties of graphene, micromechanics

1 Introduction

The linear elastic response of graphene is isotropic resulting from the six-fold rotational symmetry of hexagonal lattice [1,2]. However, many studies in simulations and experiments have observed that graphene exhibits remarkable mechanical anisotropy in the nonlinear elastic regime due to the strain-induced symmetry breaking. First-principles calculations demonstrated that the difference of tensile strength and strain to failure of graphene along the armchair and zigzag directions are as high as 10% and 37%, respectively [3]. Molecular dynamics simulations revealed that the propagation of transverse acoustic wave with frequency over 3 THz in graphene is chirality-dependent [4]. Gao et al. [5] demonstrated anisotropic tearing behaviors of graphene during mechanical exfoliation by using atomistic simulations. Theoretically, Liu et al. [6] derived an analytical formula of the energy for arbitrary graphene edge, and the energy difference between the armchair and zigzag edges obtained from first-principles calculations is about 17%. Experimentally, Kim et al. [7] investigated the crystallographic orientations of graphene tears using transmission electron microscopy, and they observed that edges from mechanically induced ripping exhibit straight lines that are predominantly aligned along the armchair or zigzag directions.

Multilayer graphene, a typical layered crystal, also exhibits exceptional anisotropic mechanical behaviors [8,9]. For example, molecular simulations demonstrate that the mechanical properties of multilayer graphene are insensitive to the layer numbers, and the mechanical anisotropy of graphene is transferred into their multilayer assemblies [9]. In experiments, Lee et al. reported the high-strain-rate behavior of multilayer graphene over a wide range of thicknesses (10–100 nm) by using miniaturized ballistic tests, which shows that the initiation of radial cracks approximately follows crystallographic directions and extends outward well beyond the impact area [8]. This strong mechanical anisotropy would induce strain localization of chemical bonds and thus premature cracks along weak planes [6], which could significantly reduce its mechanical performance for loading-bearing uses in engineering applications, such as the reinforced phase in composites and ballistic protection.

It is well known that material properties can be engineered by tailoring the structures, and hence a few studies have been conducted to tune the mechanical anisotropy and relevant properties of graphene based on this principle [10–17]. Fang et al. [18] measured the mechanical anisotropy degree of graphene as a function of tensile strain, indicating the strain-induced tuning of mechanical anisotropy. Dong et al. [19] demonstrated that the mechanical anisotropy in graphene can be regulated by introducing defects, such as holes and cracks. However, a universal strategy of widely tuning the inherited mechanical anisotropy in multilayer graphene without damaging the sp^2 nature of graphene has not been developed.

In this work, we find that the mechanical anisotropy in multilayer graphene can be efficiently tuned via interlayer twist. First, the orientation-dependent mechanical behaviors of monolayer graphene are described in an analytical formula based on the atomistic simulations. Furthermore, the analytical formula is generalized for predicting the mechanical anisotropy in twisted multilayer graphene, which is supported by direct atomistic simulations. It is concluded that the strong nonlinear mechanical anisotropy in multilayer graphene can be tuned and even eliminated by modulating the interlayer twist angle. Finally, the strategy is generalized for tuning the mechanical anisotropy of other layered crystals.

2 Materials and Methods

We constructed periodic rectangular cells with two edges along x and y direction, respectively, for monolayer and bilayer graphene with different configurations, which are then subjected to a tensile load along x direction (Fig. 1). Notably, the size of minimum periodic rectangular cells for computations depends on the orientation

[1]Corresponding authors.

Contributed by the Applied Mechanics Division of ASME for publication in the Journal of Applied Mechanics. Manuscript received August 21, 2020; final manuscript received September 30, 2020; published online October 27, 2020. Assoc. Editor: Yashashree Kulkarni.

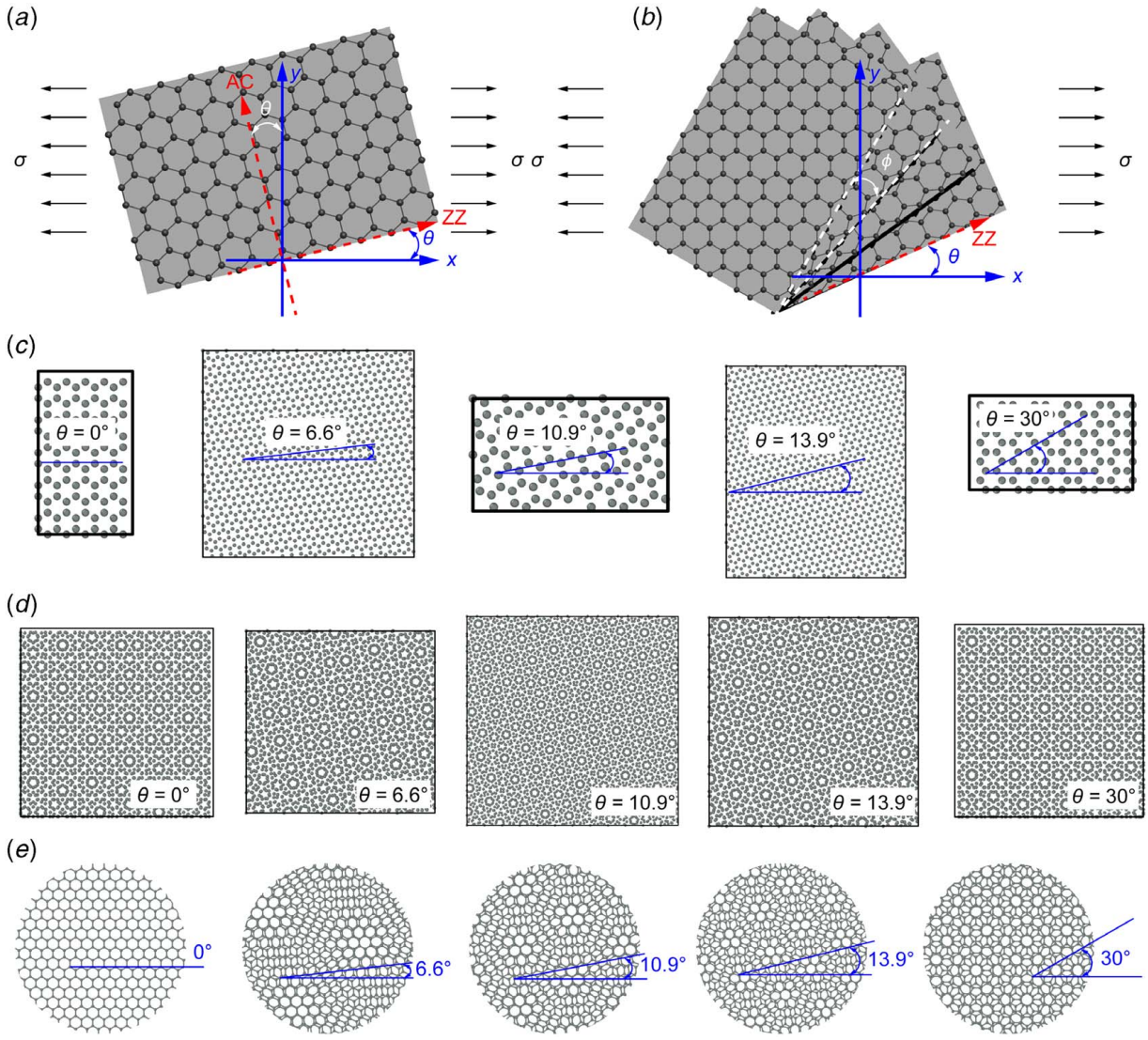

Fig. 1 (*a*) Illustration of graphene monolayer oriented in a way that the angle between the zigzag direction and the *x*-axis is θ. The load is applied along *x*-axis. (*b*) Illustration of multilayer graphene oriented in a way that the angle between the zigzag direction of bottom graphene layer and the *x*-axis is θ, and the interlayer is twisted by an angle (ϕ). The load is applied along *x*-axis. (c) Periodic rectangular cells of monolayer graphene with different θ. (*d*) Rectangular cells of bilayer graphene with ϕ of 30 deg and different θ. (*e*) Typical Moiré Patterns in graphene bilayer with ϕ of 0 deg, 6.6 deg, 10.9 deg, 13.9 deg, and 30 deg, respectively.

angle (θ), interlayer twist angle (ϕ), and layer number (n). As illustrated in Fig. 1(*a*), the graphene lattice is oriented in a way that the angle between the zigzag direction and the *x*-axis is θ. For twisted multilayer graphene, θ is defined as the angle between the zigzag direction of bottom graphene layer and the *x*-axis, and ϕ is the interlayer twist angle between the adjacent layers (Fig. 1(*b*)). The constructed periodic rectangular cells of monolayer graphene with different θ are shown in Fig. 1(*c*), and periodic rectangular cells of bilayer graphene with different ϕ and θ were constructed by matching the lattice constants of two layers. For example, the computational cells of bilayer graphene with ϕ of 30 deg and θ of 0 deg, 6.6 deg, 10.9 deg, 13.9 deg, and 30 deg, respectively, are shown in Fig. 1(*d*). Typical Moiré Patterns are observed in twisted graphene bilayers with ϕ of 0, 6.6, 10.9, 13.9, and 30 deg, respectively (Fig. 1(*e*)). To investigate the mechanical behaviors of graphene and multilayer graphene, molecular simulations of uniaxial tensile tests are carried out using large-scale atomic/molecular massively parallel simulator computational package [20]. To avoid the size effect of the simulations, periodic boundary conditions along the in-plane dimensions are used. Herein, the intralayer interactions are captured via the optimized Tersoff potential [21], and the interlayer interactions are modeled via a registry-dependent Kolmogorov-Crespi potential [22] recently parameterized by Ouyang and his coworkers [23]. Before the tensile deformation protocol is started, all structures of graphene and multilayer graphene are fully energy minimized using a conjugate gradient algorithm. Afterward, mechanical responses to tensile loads of these structures are investigated by uniaxially deforming the simulation box and applying affine displacement to the atomistic positions, while the transverse direction of the box is energy minimized with a conjugate gradient method to achieve the uniaxial stress state. Herein, the nominal stress–strain curves are recorded for analysis. Unless other noted, all samples are uniaxially stretched along *x*-axis (Figs. 1(*a*) and 1(*b*)).

3 Results and Discussion

3.1 Orientation-dependent Mechanical Behaviors of Monolayer Graphene. First, the mechanical behaviors of monolayer graphene as a function of θ are investigated by using molecular calculations. When $\theta = 0$ deg and 30 deg, the mechanical

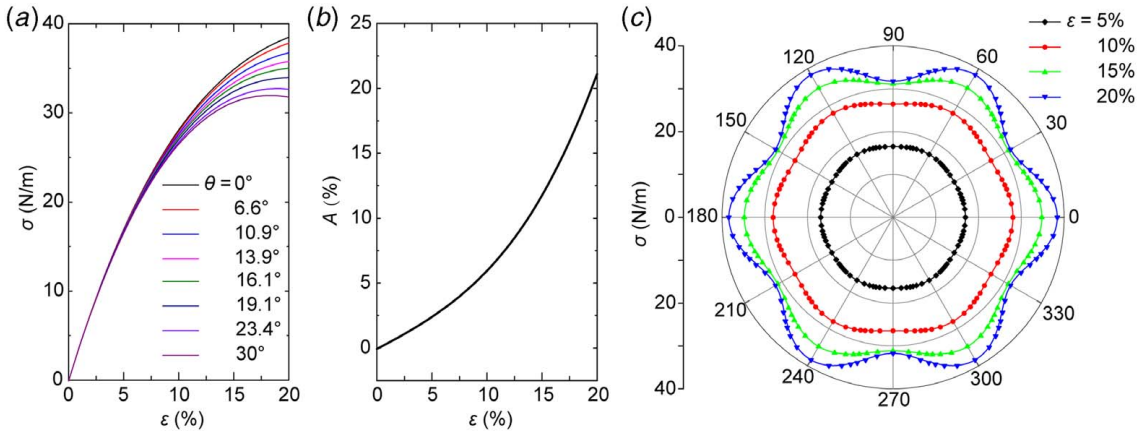

Fig. 2 (*a*) Stress–strain curves of graphene oriented along different directions subjected to tensile loads. (*b*) Mechanical anisotropy of graphene as a function of tensile strain (Eq. (1)). (c) Orientation-dependent mechanical responses of graphene subjected to different magnitude of tensile strain as a function of θ. The dots and lines are from the simulations and predictions, respectively.

behaviors of the armchair and zigzag planes are determined by the loading along the zigzag and armchair directions, respectively. The stress–strain curves of pristine graphene with different θ are shown in Fig. 2(*a*). It can be found that mechanical responses and deformation of graphene oriented along different directions yield significant difference as the strain increases. For example, the maximum difference between tensile strength is as high as 25%. Herein, we define the mechanical anisotropy degree as the difference between maximum stress and minimum stress of graphene oriented along different directions when the same magnitude of tensile strain is applied

$$A(\varepsilon) = \max_{\theta} \sigma(\varepsilon) / \min_{\theta} \sigma(\varepsilon) - 1 \tag{1}$$

As shown in Fig. 2(*b*), it can be found that the mechanical anisotropy degree increases with the increasing of tensile strain, suggesting the strain-induced tuning of the mechanical anisotropy in graphene monolayer.

Furthermore, we found that the calculated stress–strain curves of graphene oriented along different directions can be approximated in analytical form by simply capturing the six-fold rotational symmetry of graphene

$$\sigma_1(\varepsilon, \theta) = \frac{\sigma(\varepsilon, 0 \text{ deg}) + \sigma(\varepsilon, 30 \text{ deg})}{2} + \frac{\sigma(\varepsilon, 0 \text{ deg}) - \sigma(\varepsilon, 30 \text{ deg})}{2} \cos(6\theta) \tag{2}$$

where $\sigma(\varepsilon, 0 \text{ deg})$ and $\sigma(\varepsilon, 30 \text{ deg})$ are the stress–strain curves of graphene stretched along the zigzag and armchair directions, respectively. The analytical formula shows that the stress response of graphene under the same magnitude of strain is a function of θ with a period of 60 deg.

To verify the reliability of Eq. (2) for describing the stress–strain curves of graphene monolayer, a series of tensile strains are applied on graphene oriented along different directions and the resulted stress responses are recorded. It can be found that the simulations agree with the analytical curves (Fig. 2(*c*)), and the maximum deviation between predictions and simulations is less than 0.8%, indicating the sufficient robustness of Eq. (2) in capturing the tensile stress–strain behaviors of graphene monolayer.

3.2 Mechanical Anisotropy of Twisted Multilayer Graphene. Furthermore, we explore the mechanical anisotropy in graphene bilayer with varying interlayer twist angles (ϕ). Without considering the contribution of interlayer weak interaction, which is reasonable since the experimentally measured low binding energy and superlubric sliding between twisted graphene layers [24,25], the analytical stress–strain curves of twisted bilayer graphene can thus be derived from Eq. (2) based on the principle of linear superposition of the stretching forces in the two layers

$$\sigma_2(\varepsilon, \theta) = \frac{\sigma_1(\varepsilon, \theta) + \sigma_1(\varepsilon, \theta + \phi)}{2} \tag{3}$$

It can be found here that that there is a "phase shift" of ϕ between the stress responses of two layers in Eq. (3). This phase shift is induced by the interlayer twist and it can be used to tune the

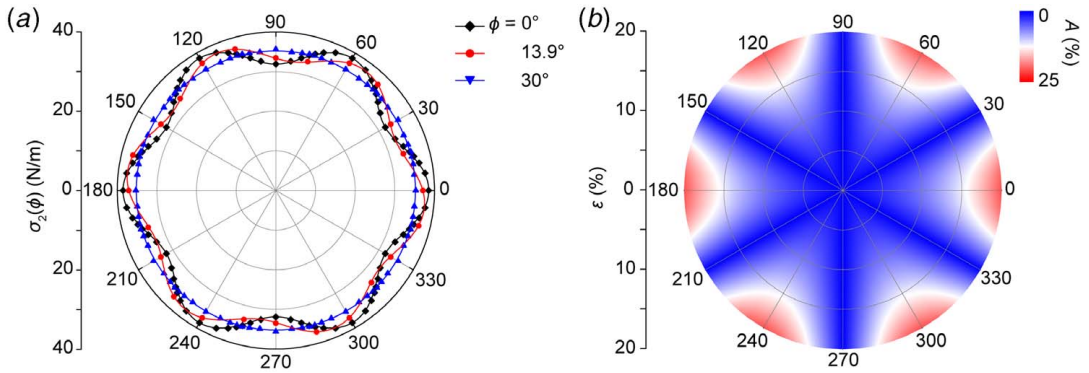

Fig. 3 (*a*) Stress distribution of twisted bilayer graphene under tensile strain of 20% as a function of θ. The lines are from theoretical predictions and the dots are from direct simulations. (*b*) The mechanical anisotropy degree of bilayer graphene as a function of ε and ϕ.

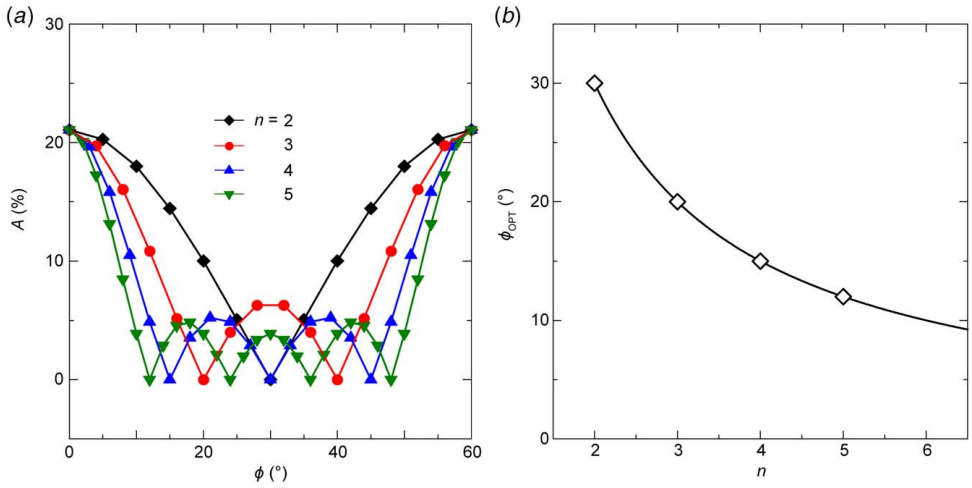

Fig. 4 (*a*) Mechanical anisotropy degree in multilayer graphene as a function of ϕ. (*b*) Optimal interlayer twist angle to minimize the mechanical anisotropy as a function of *n*.

orientation-dependent mechanical responses of bilayer graphene, which will be discussed in more detail.

To verify the reliability of Eq. (3) in predicting the stress–strain curves of twisted bilayer graphene, we construct representative models of twisted bilayer graphene oriented along different directions (Fig. 1(*b*)) and then the orientation-dependent stress responses under tensile strain of 20% are measured as shown in Fig. 3(*a*). It can be found that the direct atomistic simulations of twisted graphene bilayer are in good consistence with the theoretical prediction, and the maximum deviation is less than 0.8%, indicating the high reliability of the analytical formula in depicting the stress–strain curves of bilayer graphene. Meanwhile, it suggests that the interlayer weak interaction that has been neglected in the derivation of Eq. (3) almost does not affect the mechanical responses. More importantly, it is found that the mechanical anisotropy degree decreases as ϕ increases from 0 deg to 30 deg (Fig. 3(*a*)). Notably, the mechanical anisotropy degree of graphene under arbitrary strain is reduced to 0% when $\phi = \pi/6 + n\pi/3$, $n = 0, 1, 2\ldots$ (Fig. 3(*b*)). These findings demonstrate that the mechanical anisotropy in bilayer graphene can be effectively tuned by controlling the interlayer twist angle.

Similarly, the stress–strain curves of twisted multilayer graphene can be generalized as

$$\sigma_n(\varepsilon, \theta) = \frac{\sum_1^n \sigma_1[\varepsilon, \theta + (i-1)\phi]}{n} \tag{4}$$

where n is the layer number. Based on Eqs. (1) and (4), the maximum mechanical anisotropy degree of twisted multilayer graphene with different n and ϕ is shown in Fig. 4(*a*). It demonstrates that maximum anisotropy degree is a periodic function of ϕ with a period of 60 deg. In addition, there are $n-1$ points of special interlayer twist angles within 60 deg that make multilayer graphene exhibit the mechanical anisotropy degree of zero, which indicates that there are more twisted phases of multilayer graphene to eliminate the mechanical anisotropy with the increasing of n. Herein, we define the minimum interlayer twist angle that could maximally reduce the mechanical anisotropy degree as an optimal interlayer twist angle (ϕ_{OPT}), which is derived from Eq. (4) as a function of n

$$\phi_{\mathrm{OPT}} = \frac{60 \text{ deg}}{n} \tag{5}$$

In theory, the mechanical anisotropy degree is reduced to 0% for twisted phases of multilayer graphene with ϕ_{OPT}, and ϕ_{OPT} decreases with the increase of n in multilayer graphene (Fig. 4(*b*)). It indicates that the more n increases, the smaller

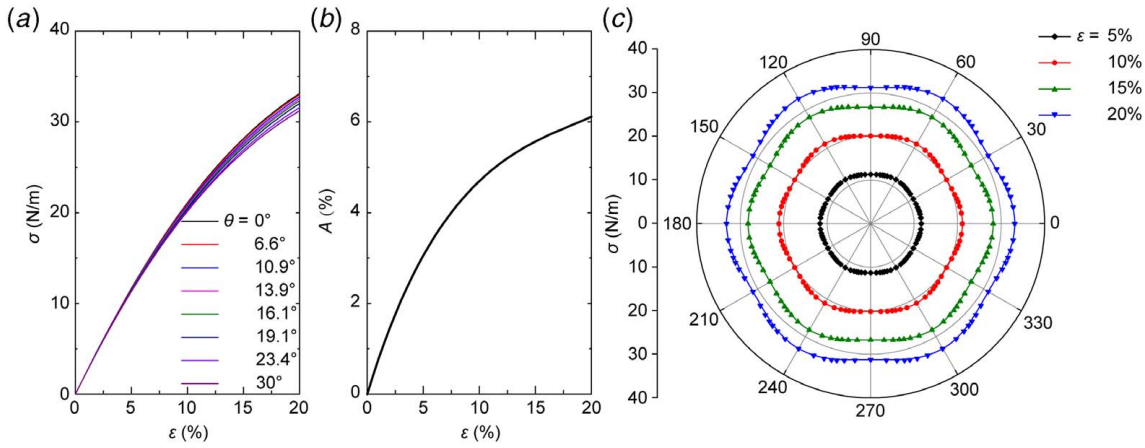

Fig. 5 (*a*) Stress–strain curves of *h*-BN oriented along different directions subjected to tensile loads. (*b*) Mechanical anisotropy of *h*-BN as a function of tensile strain (Eq. (1)). (*c*) Orientation-dependent mechanical responses of *h*-BN subjected to different magnitude of tensile strain as a function of θ. The dots and lines are from the simulations and predictions, respectively.

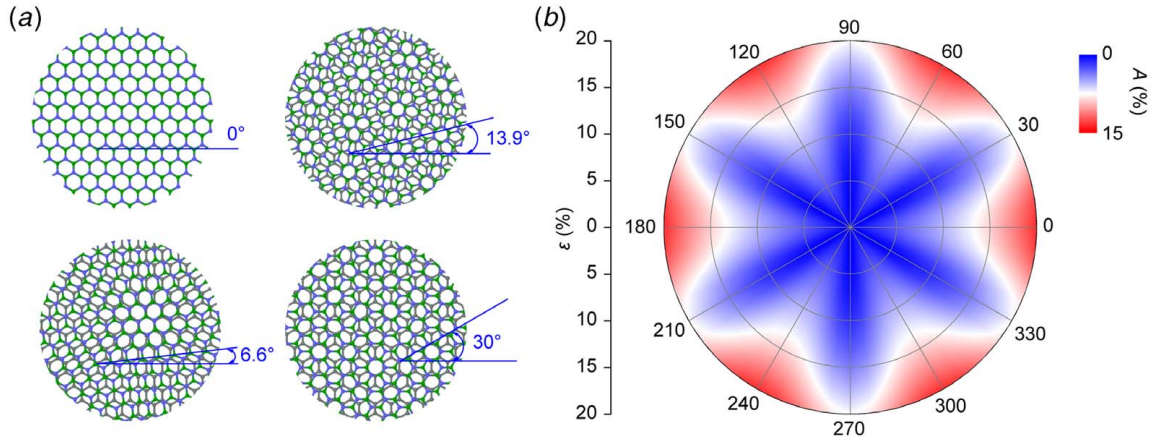

Fig. 6 (*a*) Typical Moiré Patterns in bilayer graphene/*h*-BN heterojunctions with ϕ of 0 deg, 6.6 deg, 13.9 deg, and 30 deg, respectively. (*b*) The mechanical anisotropy degree of bilayer graphene/*h*-BN heterojunctions as a function of ε and ϕ.

interlayer twist perturbation is needed to completely eliminate the mechanical anisotropy. These findings show that the strong nonlinear mechanical anisotropy emerging in multilayer graphene can be widely tuned by interlayer twist.

3.3 Generalized Strategy for Tuning the Mechanical Anisotropy of Other Layered Crystals. Finally, we generalize this strategy for tuning the mechanical anisotropy of other layered crystals. Herein, we selected another two-dimensional (2D) material as hexagonal boron nitride (*h*-BN). The stress–strain curves of monolayer *h*-BN with different θ are shown in Fig. 5(*a*). With B and N atoms in a hexagonal lattice, *h*-BN has a three-fold symmetry, and so does bilayer graphene/*h*-BN. Similar to graphene monolayer, it can be found that the mechanical anisotropy degree increases as the tensile strain increases (Fig. 5(*b*)). Figure 5(*c*) shows the orientation-dependent mechanical responses of *h*-BN subjected to different magnitude of tensile strain as a function of θ. The maximum deviation between predictions and simulations is less than 0.9%, indicating the reliability of the strategy for capturing the tensile stress–strain behaviors of monolayer *h*-BN. Combining the above-calculated stress–strain curves of 2D materials with different θ and the proposed theory, the stress–strain curves of homogeneous or heterogeneous multilayer of graphene and *h*-BN can be predicted. Here, we explore the mechanical anisotropy of twisted bilayer graphene/*h*-BN heterojunctions (Fig. 6(*a*)). Figure 6(*b*) shows the mechanical anisotropy degree of this heterojunction with different interlayer twist angle under arbitrary strain. The nonlinear mechanical anisotropy of this layered heterojunction can be also greatly modulated by interlayer twist. For example, the anisotropy degree of graphene/*h*-BN heterojunction is only 7.35% at strain of 20% and ϕ of 30 deg, which is much smaller than that of ϕ of 0 deg.

4 Conclusion

In summary, the mechanical anisotropy of twisted layered graphene is formulated by a continuum theory and then supported by atomistic simulations. It is found that the strong nonlinear mechanical anisotropy in multilayer graphene can be widely tuned and even eliminated by modulating the interlayer twist angle between adjacent layers. Finally, the strategy is generalized for tuning the mechanical anisotropy of other layered crystals. Our work outlines an efficient strategy of tuning the strong nonlinear mechanical anisotropy in multilayer graphene and other layered crystals by interlayer twist.

Acknowledgment

This work was supported by the National Natural Science Foundation of China (11902225) and the Natural Science Foundation of Hubei Province (2019CFB174). The numerical calculations in this work have been done on the supercomputing system in the Supercomputing Center of Wuhan University.

Conflict of Interest

There are no conflicts of interest.

Data Availability Statement

The datasets generated and supporting the findings of this article are obtainable from the corresponding author upon reasonable request.

References

[1] Li, R., Shao, Q., Gao, E., and Liu, Z., 2020, "Elastic Anisotropy Measure for Two-Dimensional Crystals," Extreme Mech. Lett., **34**, p. 100615.
[2] Zhang, C., Wei, N., Gao, E., and Sun, Q., 2020, "Poisson's Ratio of Two-Dimensional Hexagonal Crystals: A Mechanics Model Study," Extreme Mech. Lett., **38**, p. 100748.
[3] Liu, F., Ming, P. M., and Li, J., 2007, "Ab Initio Calculation of Ideal Strength and Phonon Instability of Graphene Under Tension," Phys. Rev. B, **76**(6), p. 064120.
[4] Liu, X. Y., Wang, F. C., and Wu, H. A., 2013, "Anisotropic Propagation and Upper Frequency Limitation of Terahertz Waves in Graphene," Appl. Phys. Lett., **103**(7), p. 071904.
[5] Gao, E., Lin, S., Qin, Z., Buehler, M., Feng, X., and Xu, Z., 2018, "Mechanical Exfoliation of Two-Dimensional Materials," J. Mech. Phys. Solids, **115**, pp. 248–262.
[6] Liu, Y., Dobrinsky, A., and Yakobson, B. I., 2010, "Graphene Edge From Armchair to Zigzag: The Origins of Nanotube Chirality?" Phys. Rev. Lett., **105**(23), p. 235502.
[7] Kim, K., Artyukhov, V. I., Regan, W., Liu, Y., Crommie, M. F., Yakobson, B. I., and Zettl, A., 2012, "Ripping Graphene: Preferred Directions," Nano Lett., **12**(1), pp. 293–297.
[8] Lee, J.-H., Loya, P. E., Lou, J., and Thomas, E. L., 2014, "Dynamic Mechanical Behavior of Multilayer Graphene via Supersonic Projectile Penetration," Science, **346**(6213), pp. 1092–1096.
[9] Zhang, Y. Y., and Gu, Y. T., 2013, "Mechanical Properties of Graphene: Effects of Layer Number, Temperature and Isotope," Comp. Mater. Sci., **71**, pp. 197–200.
[10] Choi, J. S., Kim, J.-S., Byun, I.-S., Lee, D. H., Lee, M. J., Park, B. H., Lee, C., Yoon, D., Cheong, H., Lee, K. H., Son, Y.-W., Park, J. Y., and Salmeron, M., 2011, "Friction Anisotropy-Driven Domain Imaging on Exfoliated Monolayer Graphene," Science, **333**(6042), pp. 607–610.
[11] Qi, Z., Campbell, D. K., and Park, H. S., 2014, "Atomistic Simulations of Tension-Induced Large Deformation and Stretchability in Graphene Kirigami," Phys. Rev. B, **90**(24), p. 245437.

[12] Wei, N., Chen, Y., Cai, K., Zhao, J., Wang, H.-Q., and Zheng, J.-C., 2016, "Thermal Conductivity of Graphene Kirigami: Ultralow and Strain Robustness," Carbon, **104**, pp. 203–213.
[13] Hua, Z., Zhao, Y., Dong, S., Yu, P., Liu, Y., Wei, N., and Zhao, J., 2017, "Large Stretchability and Failure Mechanism of Graphene Kirigami Under Tension," Soft Matter, **13**(47), pp. 8930–8939.
[14] López-Polín, G., Ortega, M., Vilhena, J. G., Alda, I., Gomez-Herrero, J., Serena, P. A., Gomez-Navarro, C., and Pérez, R., 2017, "Tailoring the Thermal Expansion of Graphene via Controlled Defect Creation," Carbon, **116**, pp. 670–677.
[15] Gao, E., and Xu, Z., 2015, "Thin-Shell Thickness of Two-Dimensional Materials," ASME J. Appl. Mech., **82**(12), p. 121012.
[16] Qin, H., Sorkin, V., Pei, Q.-X., Liu, Y., and Zhang, Y.-W., 2020, "Failure in Two-Dimensional Materials: Defect Sensitivity and Failure Criteria," ASME J. Appl. Mech., **87**(3), p. 030802.
[17] Volokh, K. Y., 2012, "On the Strength of Graphene," ASME J. Appl. Mech., **79**(6), p. 064501.
[18] Fang, Y., Wang, Y., Imtiaz, H., Liu, B., and Gao, H., 2019, "Energy-Ratio-based Measure of Elastic Anisotropy," Phys. Rev. Lett., **122**(4), p. 045502.
[19] Dong, S., Xia, Y., Huang, R., and Zhao, J., 2020, "Modulating Mechanical Anisotropy of Two-Dimensional Materials by Controlling Their Defects," Carbon, **158**, pp. 77–88.
[20] Plimpton, S., 1995, "Fast Parallel Algorithms for Short-Range Molecular Dynamics," J. Comput. Phys., **117**(1), pp. 1–19.
[21] Lindsay, L., and Broido, D. A., 2010, "Optimized Tersoff and Brenner Empirical Potential Parameters for Lattice Dynamics and Phonon Thermal Transport in Carbon Nanotubes and Graphene," Phys. Rev. B, **81**(20), p. 205441.
[22] Kolmogorov, A. N., and Crespi, V. H., 2005, "Registry-Dependent Interlayer Potential for Graphitic Systems," Phys. Rev. B, **71**(23), p. 235415.
[23] Ouyang, W., Mandelli, D., Urbakh, M., and Hod, O., 2018, "Nanoserpents: Graphene Nanoribbon Motion on Two-Dimensional Hexagonal Materials," Nano Lett., **18**(9), pp. 6009–6016.
[24] Liu, Z., Yang, J., Grey, F., Liu, J. Z., Liu, Y., Wang, Y., Yang, Y., Cheng, Y., and Zheng, Q., 2012, "Observation of Microscale Superlubricity in Graphite," Phys. Rev. Lett., **108**(20), p. 205503.
[25] Liu, Z., Liu, J. Z., Cheng, Y., Li, Z., Wang, L., and Zheng, Q., 2012, "Interlayer Binding Energy of Graphite: A Mesoscopic Determination From Deformation," Phys. Rev. B, **85**(20), p. 205418.